

Design of an Ultrasonic Micro-Array for Near Field Sensing during Retinal Microsurgery

Clyde Clarke

Dept. of Electrical and Computer Engineering
Morgan State University
Baltimore, MD, USA
clyde.clarke@gmail.com

Ralph Etienne-Cummings

Dept. Electrical and Computer Engineering
Johns Hopkins University
Baltimore, MD, USA
retienne@jhu.edu

Abstract— A method for obtaining the optimal and specific sensor parameters for a tool-tip mountable ultrasonic transducer micro-array is presented. The ultrasonic transducer array sensor parameters, such as frequency of operation, element size, inter-element spacing, number of elements and transducer geometry are obtained using a quadratic programming method to obtain a maximum directivity while being constrained to a total array size of 4 mm^2 and the required resolution for retinal imaging. The technique is used to design a uniformly spaced $N \times N$ transducer array that is capable of resolving structures in the retina that are as small as $2 \text{ }\mu\text{m}$ from a distance of $100 \text{ }\mu\text{m}$. The resultant 37×37 array of $16 \text{ }\mu\text{m}$ transducers with $26 \text{ }\mu\text{m}$ spacing will be realized as a Capacitive Micromachined Ultrasonic Transducer (CMUT) array and used for imaging and robotic guidance during retinal microsurgery.

I. INTRODUCTION

Tool-tip mounted micro ultrasonic imagers and proximity detectors have been on the “wish-list” of retinal microsurgeons for some time. Such a tool is a high priority because current methods, involving external optical microscopy and individual “feel,” provide insufficient information, relegating the performance of retinal microsurgery to a handful of super specialized and highly skilled surgeons. Unfortunately, treating a growing aging population will require a large number of these specialists, so any tool that will help improve the skills of *any* microsurgeon will be a huge benefit to society. The micro-array described designed in this paper will make some inroads towards this goal.

The retinal tissue consists of layered structures of spatially varying density and compressibility [7] that present a challenging environment for ultrasonic imaging. In cases where surgery has to be performed on regions of macular degeneration, a leading cause of loss of vision in the elderly, these structures are on the order of $2 \text{ }\mu\text{m}$ and are located beneath multiple layers of macular tissue. Here we present a technique that will allow us to design ultrasonic micro-arrays for *near-field* imaging of the retinal area. The micro-sensor array characteristics, such as transducer and array size, frequency, are directly optimized to obtain the maximum directivity and resolution in the intra-vitreous region. We target a uniformly $N \times N$ transducer array with a total size of

$2 \text{ mm} \times 2 \text{ mm}$. The total size will allow it to be mounted on a tool that will be inserted into the eye. In addition to imaging, the micro-array will also measure the proximity and the relative orientation of the tool to the retina (to avoid inadvertent damage). See Fig. 1 for an illustration of the system.

We are developing this ultrasonic micro-array for macular degeneration intervention. Macular degeneration is classified in two forms. Wet Macular Degeneration is caused by the growth of new abnormal blood vessels from the choroidal neovascularization (CNV). Abnormal blood vessels first leak fluid under the macula, then form scar tissue leading to central vision loss. In dry macular degeneration, a yellow deposit called drusen forms beneath the retina. When present for a long time, drusen may cause the macula to thin and stop functioning.

There are significant advantages in using ultrasonic arrays as a diagnostic tool for locating regions of macular degeneration. Firstly, ultrasonic imaging presents an ideal imaging modality because ultrasonic waves are able to penetrate beneath the layers of the retina, revealing disparities in the spatial density and compressibility of the macular tissue. Secondly, the delicate and complex nature of motions required for retinal microsurgery are complicated by the relative lack of proprioceptive feedback [8]. The ability for surgeons to determine the proximity and orientation of their tools relative to the retinal surface is facilitated by the ranging capabilities of the ultrasonic transducer micro-array. Lastly, imaging the retina in the near-field of the ultrasonic imager, presents a significant increase in resolution compared to other far-field imaging techniques. An illustration of the tool-mounted system is shown in Fig. 1.

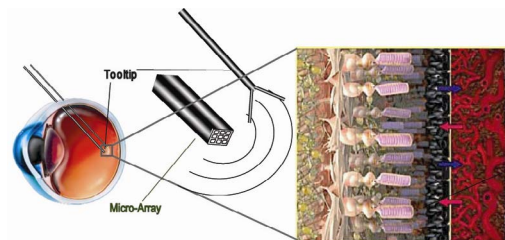


Figure 1. Retinal Microsurgical System: An example of a tool-mounted ultrasonic micro-array, a micro-tweezer and a cross-section of layers of the retina

II. DIRECTIVITY AND ARRAY FACTOR

A. Array Factor

Given the average size of the macular region it is necessary to find the angular resolution of the radiation pattern for a given transducer array geometry. An isotropic point source has no directionality therefore it radiates uniformly in all directions. The introduction of additional isotropic components increases the directionality of the radiation increasing the spatial resolution. A linear array is an array of components that are equally spaced. The array factor, $A(\psi)$ derived in [1] for a linear array, is a function of the number of elements and their spacing, is used obtain an azimuthal radiation pattern. The disadvantage of the linear array is that it leads to a non-directional radiation pattern in the elevation of the array. To improve the directionality in both the azimuthal and elevation a planar array is introduced to provide a significant reduction in the overall size of the transducer array as well as providing a directed radiation pattern in both the azimuthal and elevation directions of the array. The array factor determines the radiation pattern of an array. The array factor of an $N \times N$ uniformly spaced array is given in equation (1)

$$AF(\psi) = \left[\frac{1}{N} \frac{\sin\left(N \frac{\psi_x}{2}\right)}{\sin\left(\frac{\psi_x}{2}\right)} \right] \left[\frac{1}{N} \frac{\sin\left(N \frac{\psi_y}{2}\right)}{\sin\left(\frac{\psi_y}{2}\right)} \right] \quad (1)$$

The variable N defines the number of elements along an axis of the array. The variables ψ_x and ψ_y are the digital wavenumber in the x and y directions, given in equations (2) and (3).

$$\psi_x = kd_x \sin(\theta) \cos(\varphi) \quad (2)$$

$$\psi_y = kd_y \cos(\theta) \cos(\varphi) \quad (3)$$

Where d_x and d_y are the inter-element spacing in the x and y directions. The elevation and azimuthal angles are given by θ and φ respectively.

B. Element Pattern

The far-zone field (the region of the field of an antenna where the angular field distribution is essentially independent of the distance from the antenna) of an array of identical elements is equal to the product of the field of a single element and the array factor. The element pattern of the single element changes the directivity of the array. King and Wong [2] have calculated the directivity of $N \times N$ planar arrays. In this work an element pattern of rectangular aperture, to be more compatible with VLSI/MEMS fabrication [6], of width W and length L is used to obtain the overall radiation pattern of the array. The values of L and W are set equal to simplify the optimization process. The directivity function of the rectangular aperture is given in [4]

C. Array Directivity

The directivity is the ratio of an isotropic source W/sr (watts per steradian) over that of the maximum radiation intensity W/sr of the source. The field pattern of an $N \times N$ planar array with uniform distribution is given in [3]. Using the element pattern of a square aperture and the array factor of a planar array (1), the overall field pattern is derived using the product rule. The resulting field pattern is given in equation (4).

$$E(\theta, \varphi) = E_e(\theta, \varphi) \left[\frac{1}{N} \frac{\sin\left(N \frac{\psi_x}{2}\right)}{\sin\left(\frac{\psi_x}{2}\right)} \right] \left[\frac{1}{N} \frac{\sin\left(N \frac{\psi_y}{2}\right)}{\sin\left(\frac{\psi_y}{2}\right)} \right] \quad (4)$$

Where $E_e(\theta, \varphi)$ is the element radiation pattern. The total directivity is determined by integration of the power pattern over the visible space ($0 \leq \theta \leq \pi/2$) since the radiation in the region ($\pi/2 \leq \theta \leq \pi$) is assumed to be zero. The directivity is expressed, as equation (5) [3].

$$D = \frac{4\pi}{\int_0^{2\pi} \int_0^{\pi/2} E^2(\theta, \varphi) \sin(\theta) d\theta d\varphi} \quad (5)$$

Steering of the array off broadside will introduce a broader beamwidth that increases proportionally toward endfire of the array. The minimum achievable beamwidth occurs when the radiation pattern is steered broadside to the array. Steering off broadside will cause the directivity to decrease from the maximum achievable value from that of (6).

III. OPTIMIZATION TECHNIQUE

A. Optimization Methodology

The objective of the optimization technique is to obtain the maximum directivity of a uniformly excited $N \times N$ transducer array constrained to a size of $2 \text{ mm} \times 2 \text{ mm}$. The parameters of element size, inter-element spacing, and number of elements are all adjusted during the optimization process to obtain the maximum directivity at frequencies of operation ranging from 1 MHz to 35 MHz. Much work has been done to characterize retinal tissues in the range of frequencies of 50 MHz to 100 MHz in the work of Ye [3]. The frequencies chosen for simulation are used to satisfy the requirement of a minimal edge spacing of $10 \mu\text{m}$. The frequency that produces the maximum directivity is then considered to be the uniformly excited array that can produce the best resolution out of the set of all possible arrays. This array is then compared to the required resolution of $2 \mu\text{m}$. The operating frequency is the limiting factor in determining the inter-element spacing, element size, number of array elements. If the inter-element spacing of the transducer array is greater than $\lambda/2$ grating lobes will be produced causing interference in regions located outside of the main beam. The wavelengths that limit inter-element distances are derived from the sound speed in the vitreous humor. This assures that the transducer will operate correctly once immersed within this medium. For each frequency (wavelength) of operation the quadratic programming method is constrained within a search space that is a function of frequency.

If the length of the array is $L = 2$ mm and the minimum edge spacing of the transducer elements is α then the maximum number of elements is given in equation (6)

$$N = \left(\frac{L - \alpha}{\alpha + d_x} \right) \quad (6)$$

Following this line of reasoning the constraints on the element size, inter-element spacing and number of elements are given in (7).

$$\begin{aligned} 1 \leq N &\leq \left(\frac{L - \alpha}{\alpha + d_x} \right) \\ \alpha &\leq d_x \leq \lambda/2 \\ \alpha &\leq W \leq (\lambda/2) - \alpha \end{aligned} \quad (7)$$

Where W is the element size, N is the number of elements and d_x is the center to center spacing of the square elements. The quadratic programming technique is used to find the parameters within the constraints (7) that maximize the objective function (5) for a range of frequencies. The minimum edge spacing of $10 \mu\text{m}$ limits the usable range of ultrasonic frequencies to a range from 1 MHz to 35 MHz.

B. Quadratic Programming

A linear constrained optimization problem with a quadratic objective function is called a quadratic program. The objective of the quadratic program is to find the parameters $\mathbf{x}^* \in R^n$ (where \mathbf{x} are the parameters to be optimized and n is the number of parameters) that minimizes the objective function. These vector \mathbf{x} consist of the inter-element spacing, element size and number of elements. In this case the objective function is the directivity. The mathematical statement of the problem is given in equation (8) [5] subject to the constraints in (7).

$$\begin{aligned} \text{Minimize } f(\mathbf{x}) &= \mathbf{c}\mathbf{x} + \frac{1}{2} \mathbf{x}^T \mathbf{Q}\mathbf{x} \quad (8) \\ \text{subject to } \mathbf{lb} &\leq \mathbf{x} \leq \mathbf{ub} \end{aligned}$$

Where \mathbf{c} is an n -dimensional row vector describing the coefficients of the linear terms in the objective function, and \mathbf{Q} is an $(n \times n)$ symmetric matrix describing the coefficients of the quadratic terms of the objective function. In this case \mathbf{Q} represents the overall field pattern (4) generated by the transducer array. Where \mathbf{lb} and \mathbf{ub} signify n -dimensional lower bounds (\mathbf{lb}) and upper bounds (\mathbf{ub}) that constrain the optimization procedure at each of the 100 frequencies in the range of 1 MHz to 35 MHz.

IV. RESULTS

The constrained optimization technique was used to determine the maximum directivity of an array based on the frequency of operation, the number of elements, inter-element spacing and element sizes. Plots of frequency versus inter-element spacing, element size, and number of transducers are given to illustrate their relationship to the directivity of the array.

A. Simulation

Simulations were performed using the MatLab simulation software. The directivity of the array is evaluated at 100 evenly spaced points in the range of 1 MHz to 35 MHz. For each evaluation the optimal transducer parameters within the constraints (7) with an $\alpha = 10 \mu\text{m}$ are obtained in.

The maximum directivity occurred at a frequency of approximately 28 MHz, an inter-element spacing of $26 \mu\text{m}$ and approximately 37 elements along each principal axis of the array (x and y). The directivity at this point in the solution space is 49 dB. The minimum half power beamwidth (HPBW) is achieved at the frequency of maximum directivity. The HPBW is significant in determining whether the micro-array is capable of resolving objects of $2 \mu\text{m}$. Fig. 2 illustrates the radiation pattern of two planar arrays with $N = 1$ and $N = 37$ elements respectively which are roughly the values of an isotropic point source and that of the parameters used in the optimized array. The radiation patterns are generated within the same size constraints as that of the $2 \text{ mm} \times 2 \text{ mm}$ micro-array.

The number of elements, inter-element spacing and element sizes are plotted as a function of the operating frequency. The plots in Figs. 3, 4 indicate the optimal values determined by the quadratic programming procedure in text boxes. The X value being the optimal frequency value and the Y values indicates the optimal inter-element spacing, element size and number of elements. These curves are useful aids in determining optimal values of the parameters (inter-element spacing, number of elements and element size) that will meet directivity and beamwidth requirements of a size constrained array. The inter-element spacing and edge spacing are the distances associated with the center to center spacing of the transducer and the spacing that satisfies the minimum MEMS requirement of $\alpha = 10 \mu\text{m}$ from edge to edge.

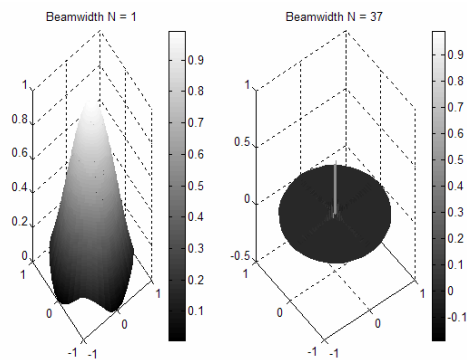


Figure 2. Micro-Array Beamwidths for $N = 1$ and $N = 37$ element arrays. The micro-array directivity is shown to increase with an increased number of elements

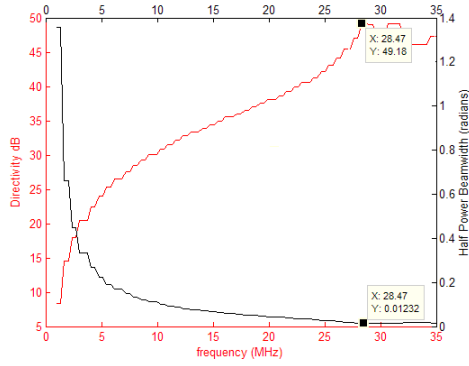


Figure 3. Directivity and Beamwidth vs Frequency: The minimum resolution value is obtained at a frequency of 28 MHz and corresponds to maximum directivity of the micro-array

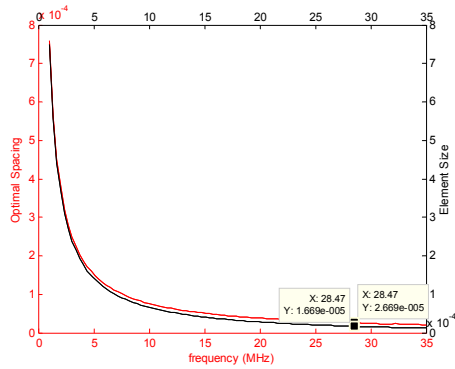


Figure 4. Inter-Element and Optimal Element Size vs Frequency. The inter-element spacing and element size are shown to decrease with frequency allowing the fabricated device to fulfill the size constraints of 4 mm^2

B. Resolution Requirements

The uniformly excited array designed from the optimization process must achieve a minimum resolution of $2 \text{ }\mu\text{m}$. Toward this end comparisons of the spatial resolution of the transducer array to that of the requirement is necessary. The angular resolution at a minimal distance of $100 \text{ }\mu\text{m}$ in the axial direction from the macular is given by (9).

$$\Delta\theta = 2 \sin^{-1}\left(\frac{M_a}{2R_a}\right) \quad (9)$$

Where M_a is the spatial resolution of $2 \text{ }\mu\text{m}$ and R_a is the axial distance measured normal the transducer array surface to the surface of the macular region. Solving for $\Delta\theta$, the angular resolution (half power beam width) for these requirements gives $\Delta\theta = 0.0200$ radians. The resolution of the transducer array was calculated using the beam solid angle Ω_a defined as “the solid angle through which all the power of the array would flow if its radiation intensity was constant” [2]. The beam solid angle is given by equation (10).

$$\Omega_a = \Theta_{1r} \Theta_{2r} = \int_0^{2\pi} \int_0^{\pi/2} E^2(\theta, \varphi) \sin(\theta) d\theta d\varphi \quad (10)$$

Where, Θ_{1r} and Θ_{2r} are the half power beamwidths in the azimuthal and elevation directions respectively. Since the array is uniform the radiation pattern is symmetric about the

azimuthal and elevation directions the beamwidths are equal. The half power beamwidth is given by the square root of (10). Θ_{1r} is 0.0123 radians which corresponds to a $1.23 \text{ }\mu\text{m}$ resolution. This value of beamwidth is well within the necessary resolution given at the minimal axial distance of $100 \text{ }\mu\text{m}$.

V. CONCLUSION

The optimal parameters needed to obtain the maximum directivity and $2 \text{ }\mu\text{m}$ resolution for a 37×37 elements, 4 mm^2 ultrasonic micro-array were obtained in Table 1.

The optimization results provide parameters that also conform to the fabrication design rules of minimum element spacing of $10 \text{ }\mu\text{m}$. The resolution of the transducer array satisfying the maximum directivity falls within the constraint of a spatial resolution of $2 \text{ }\mu\text{m}$ at $100 \text{ }\mu\text{m}$ distance away from the macular surface.

TABLE I. OPTIMIZED PARAMETERS FOR NEARFIELD RETINAL IMAGING

Optimal Parameters				
Frequency	Directivity	Element Size	Inter-Element Spacing	Number of Elements
28.42 MHz	49 dB	$16 \text{ }\mu\text{m}$	$26 \text{ }\mu\text{m}$	1369

Prior work has been done on the fabrication of ultrasonic devices called Capacitive Micromachined Ultrasonic Transducers (CMUT) [9]. CMUT’s have become an important tool in the development of ultrasonic transducer micro-arrays due to their ease of fabrication in standard microfabrication processes, along with their high sensitivity and bandwidth. Fig. 5, shows an example of a CMUT array along with its cross sectional view.

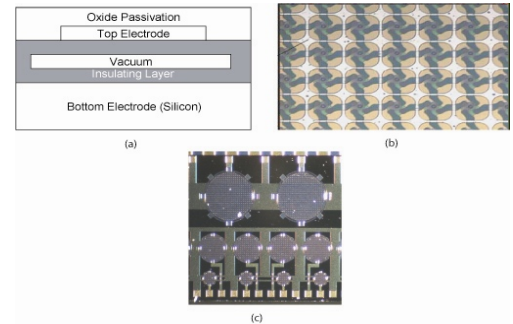


Figure 5. CMUT Array: (a) Schematic Cross Section of a CMUT cell. (b)

Magnified top view of a CMUT array of membrane diameter $12 \text{ }\mu\text{m}$ [10]. (c) CMUT fabricated at JHU These devices range in size from $100 \text{ }\mu\text{m}$ to $800 \text{ }\mu\text{m}$ [11].

REFERENCES

- [1] C.A Balanis, Antenna Theory: Analysis and Design, 2nd Edition, 1996, New York, NY: John Wiley and Sons.
- [2] H. E. King, and , J. L. Wong, “Directivity of uniformly excited $N \times N$ array of directive elements,” IEEE Trans. Antennas Propagat., vol AP-23, no.3, pp 401-404, May 1975.
- [3] D. T. Blackstock, Fundamentals of Physical Acoustics, 2000, New York, NY: John Wiley and Sons
- [4] S. G. Ye, K. A. Harasiewicz, , C. J. Palvin, and F. S. Foster, “Ultrasound Characterization of Normal Ocular Tissue in the

- Frequency Range from 50 MHz to 100 MHz," *IEEE Trans. Ultrasonics, Ferroelectrics and Frequency Control*, 1995. 42(1): p.8-14.
- [5] J. F. Bonnans, *Numerical Optimization*, 2003, Heidelberg, Berlin: Springer Verlag.
- [6] O. Oralkan, A. S Ergun, C.-H. Cheng, J.A. Hohnson, M. Karaman, T. H. Lee, and B. T. Khuri-Yakub, "Volumetric Ultrasound Imaging Using 2-D CMUT Arrays", *IEEE Trans. On UFFC*. 2003. 50(10):p 1581-15
- [7] Wollensak, G, Spoerl E, "Biomechanical Characteristics of Retina", *The Journal of Retinal and Vitreous Diseases*, 2004. Vol 24. pp 967-970
- [8] Charles, S, "Dexterity enhancement for surgery" in *Proc First Int'l Symp Medical Robotics and Computer Assisted Surgery*, 1994. 2: p 145-160
- [9] F. L. Degertekin, I. Ladabaum, J. Xuecheng, S. Calmes, B. T. Khuri-Yakub, "Fabrication and Characterization of Surface Micromachined Capacitive Ultrasonic Immersion Transducers", *IEEE Jour Micro Syst*, Vol 8, No. 1, 1999: pp 100-114
- [10] B. T. Khuri-Yakub. (2004,Oct.) Khuri-Yakub Research Group. [Online]. Available:<http://acoustics.stanford.edu/library/papers/hfcmut.pdf>
- [11] M. Clapp and Ralph Etienne-Cummings, "Ultrasonic Bearing Estimation Using a MEMS Microphone Array and Spatiotemporal Filters," *IEEE ISCAS'02*, May 2002